Original Article | **Open Access**

Extracellular Vesicles and Circulating Nucleic Acids

Li *et al. Extracell Vesicles Circ Nucleic Acids.* 2026;7:2049-67 **DOI:**10.20517/evcna.2026.126

Zinc ions inhibit migrasome biogenesis and impair platelet function by targeting cholesterol and sphingomyelin

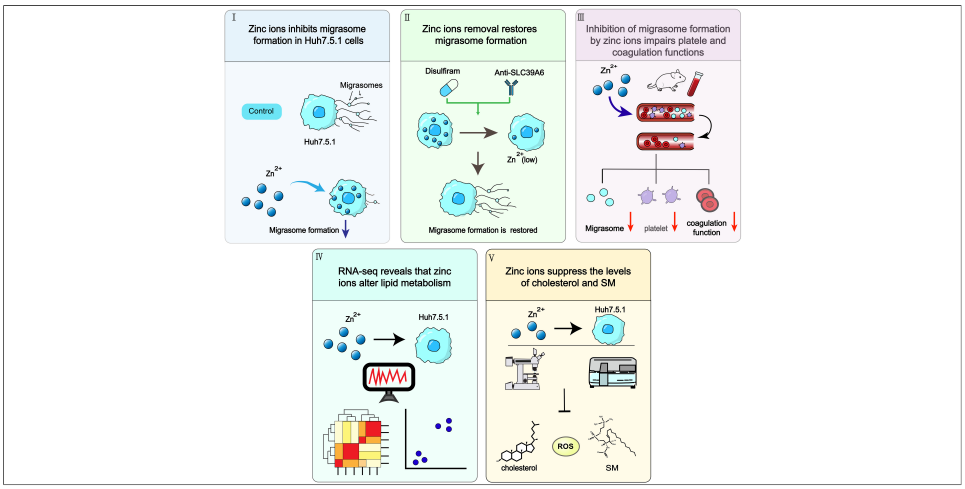
Ang Li[1,2,3], **Jingze Liu**[3], **Shuhao Zhang**[3], **Jiafeng Zhu**[3], **Leiliang Zhang**[1,3]

Keywords:
Zinc ions, migrasomes, cholesterol, platelet aggregation, sphingomyelin

Citation: Li A, Liu J, Zhang S, Zhu J, Zhang L. Zinc ions inhibit migrasome biogenesis and impair platelet function by targeting cholesterol and sphingomyelin. *Extracell Vesicles Circ Nucleic Acids.* 2026;7:2049-67. https://dx.doi.org/10.20517/evcna.2026.126

Received: 24 Jun 2026
First Decision: 31 Aug 2026
Revised: 26 Oct 2026
Accepted: 27 Oct 2026
Published: 9 Nov 2026

Academic Editor:
Yoke Peng Loh
Copy Editor:
Ting-Ting Hu
Production Editor:
Ting-Ting Hu



Abstract

Aim: Zinc ions are critical regulators of cellular homeostasis and hemostasis. Migrasomes promote thrombus formation, yet whether zinc ions influence migrasome biogenesis and the associated thrombotic outcomes remains unexplored. This work therefore examined how zinc ions affect migrasome formation and assessed the functional consequences for platelet aggregation and bleeding volume.

Methods: We performed RNA sequencing on Huh7.5.1 cells treated with $ZnSO_4$ or zinc gluconate. Migrasome formation was evaluated in both these cells and in mouse whole blood, while intracellular zinc levels were manipulated using disulfiram to enhance efflux or anti-solute carrier family 39 member 6 (SLC39A6) antibodies to inhibit uptake. Migrasomes were visualized through immunofluorescence with wheat germ agglutinin (WGA). Changes in cholesterol, sphingomyelin and reactive oxygen species (ROS) levels in response to zinc ions were measured. Migrasomes were isolated from mouse blood using a specialized isolation kit.

[1]Department of Clinical Laboratory Medicine, The First Affiliated Hospital of Shandong First Medical University & Shandong Provincial Qianfoshan Hospital, Jinan 250014, Shandong, China.
[2]School of Pharmaceutical Sciences & Institute of Materia Medica, Shandong First Medical University & Shandong Academy of Medical Sciences, Jinan 250117, Shandong, China.
[3]Department of Pathogen Biology, School of Clinical and Basic Medical Sciences, Shandong First Medical University & Shandong Academy of Medical Sciences, Jinan 250117, Shandong, China.

Correspondence to: Dr. Leiliang Zhang, Department of Pathogen Biology, School of Clinical and Basic Medical Sciences, Shandong First Medical University & Shandong Academy of Medical Sciences, Jinan 250117, Shandong, China. E-mail: armzhang@hotmail.com

Results: Zinc ions treatment reduced migrasome numbers in both cellular and whole-blood models in a dose-dependent manner. Zinc ions also decreased cholesterol, sphingomyelin, and ROS levels and impaired migrasome biogenesis. In mice, zinc administration reduced platelet counts and aggregation while increasing bleeding volume.

Conclusion: Our findings demonstrate that zinc ions modulate migrasome formation by lowering cholesterol levels, thereby negatively regulating platelet aggregation. This research enhances the current understanding of trace element biology and suggests that modulating zinc ion levels could be a potential therapeutic strategy for managing hemostatic disorders.

INTRODUCTION

Zinc, an essential trace element, plays diverse roles across a broad spectrum of biological functions. Its deficiency causes clinical symptoms such as growth retardation, delayed development, impaired wound healing, and alopecia[1]. Zinc insufficiency is also associated with increased oxidative stress[2] and accelerated cellular senescence[3].

Beyond these general roles, zinc ions actively modulate coagulation, anticoagulation, and fibrinolysis[4,5]. They bind to activated protein C and suppress its amidolytic activity, thereby inhibiting fibrinolysis[6,7]. Previous *in vitro* studies have shown that in the presence of zinc ions, fibrin gels do not undergo crosslinking, suggesting that zinc may influence the structural integrity of fibrin[8]. Additionally, zinc ions promote platelet activation, further enhancing the coagulation process[9]. Notably, at micromolar concentrations, zinc ions significantly inhibit the release of serotonin from rabbit platelets induced by platelet-activating factor and thrombin[10]. Zinc-delivering materials show enhanced hemostatic efficacy[11], and zinc-complexed rutin exerts antithrombotic effects[12].

Migrasomes are a recently identified extracellular vesicle (EV) subtype that forms on retraction fibers of migrating cells[13]. They differ from exosomes and microvesicles in both structure and biogenesis: they are single-membrane vesicles (0.5-3 μm), enriched in cholesterol and tetraspanin 4 (TSPAN4), and they bud from retraction fibers rather than multivesicular bodies[14]. These features position migrasomes within the EV field while distinguishing them as a unique, migration-dependent subtype. Intriguingly, migrasomes have been shown to actively facilitate thrombus formation[15]. In our previous work, we unexpectedly observed that physiological concentrations of zinc ions suppress migrasome formation[16], raising the possibility that zinc ions influence thrombosis at least in part through migrasome modulation.

Given the established roles of zinc in hemostasis and the emerging link between migrasomes and thrombosis, we asked whether zinc ions regulate migrasome biogenesis via cholesterol metabolism and whether such regulation affects platelet aggregation and bleeding volume *in vivo*. Here, we provide mechanistic evidence that zinc ions inhibit migrasome formation by lowering cholesterol, sphingomyelin, and reactive oxygen species (ROS) levels. These findings offer important insights into the therapeutic potential of zinc-based strategies for hemostatic disorders.

METHODS

Materials and solution preparation

Zinc sulfate ($ZnSO_4$, S22124, Shanghai Yuanye Bio-Technology, Shanghai, China) and zinc gluconate (Z100287, Shanghai Aladdin Biochemical Technology, Shanghai, China) were prepared as stock solutions at a concentration of 20 mmol/L in H_2O and stored at 4 °C. Zinc oxide nanoparticles (ZnO-NPs, 30 nm;

Z820772, Macklin, Shanghai, China) were dispersed in phosphate-buffered saline (PBS) to a final concentration of 2.5 mg/mL. The resulting suspension was vortexed for 1 min (VORTEX-5, Kylin-Bell, Haimen, China) and sonicated at 40 kHz for 20 min (SCIENTZ, Ningbo, China), after which it was kept refrigerated (4 °C) until use. Immediately before addition to the cells, the particles were vortexed for 5 min to resuspend them and then brought to the desired working dilutions with culture medium.

Plasmids and reagents

The enhanced green fluorescent protein (eGFP)-TSPAN4 [Research Resource Identifier (RRID): Addgene_210323] was supplied by Professor Li Yu from Tsinghua University. The cells were transfected with FuGENE HD (E2311, Promega, Madison, WI, USA) following the supplier's instructions. Cholesterol (HY-N0322), disulfiram (HY-B0240), and filipin complex (HY-N6716) were purchased from MedChemExpress (Princeton, NJ, USA). Wheat germ agglutinin (WGA) conjugated to fluorescein isothiocyanate (FITC) (RRID: AB_1657336, GTX01502) was supplied by GeneTex (Irvine, CA, USA). Anti-solute carrier family 39 member 6 (SLC39A6) (RRID: AB_11187270, Ab176216) was from Shanghai Aladdin Biochemical Technology (Shanghai, China). N-(6-methoxy-8-quinolyl)-p-toluenesulfonamide (TSQ) (21254, AAT Bioquest, Pleasanton, CA, USA) served as the Zn^{2+} dye.

Maintenance of cultured cells and transfection procedures

The human hepatoma line Huh7.5.1 (RRID: CVCL-E049) was supplied by Professor Francis V. Chisari from Scripps Research Institute. Cells were propagated in high-glucose Dulbecco's modified Eagle's medium (DMEM) (SH30022.01, GE Healthcare/Hyclone/whatman/Cytiva, Marlborough, MA, USA) with 10% fetal bovine serum (FBS) (FSP500, ExCell Bio, Shanghai, China), 100 U/mL penicillin, and 100 μg/mL streptomycin (SV30010, GE Healthcare/Hyclone/whatman/Cytiva, Marlborough, MA, USA). Cultures were subcultured every 2-3 days after detachment with 0.25% Trypsin-EDTA (25200-056, Gibco, Thermo Fisher Scientific, Waltham, MA, USA), with routine mycoplasma testing. Transfection was performed at about 70% confluence in a 2-cm dish using 1 μg DNA and 2.5 μL FuGENE HD.

Cell Counting Kit-8 (CCK-8) viability assay

Cells were seeded into 96-well plates at 1×10^4 cells/well and allowed to attach for 24 h. The medium was then replaced with zinc gluconate or $ZnSO_4$ at final concentrations of 0-30 μmol/L, and cells were incubated for a further 24 h. Subsequently, 10 μL CCK-8 reagent (RRID: AB_2314126, Proteintech, Wuhan, China) was added per well, followed by a 1-h incubation. Optical density was read at 450 nm on a Multiskan GO microplate reader (Thermo Fisher, USA).

Immunofluorescence staining and imaging

To visualize migrasomes, cells grown on glass coverslips (YA0350, Solarbio, Beijing, China) were fixed using 4% paraformaldehyde (P1110, Solarbio, Beijing, China) and then treated with WGA (2 μg/mL) or filipin (40 μmol/L) for 30 min. An ECHO RVL2-K microscope (RRID: SCR_026523, USA) was used to capture fluorescence images.

TSQ and WGA staining

Huh7.5.1 cells were plated in 6-well plates and maintained for 24 h before treatment. The cultures then received 20 μmol/L $ZnSO_4$ or zinc gluconate for 17 h, with untreated wells included as controls. After being rinsed twice with PBS, cells were exposed for 30 min at 37 °C under 5% CO_2 to a phenol red-free DMEM solution containing 10 μmol TSQ and 2 μg/mL WGA. Cells were then washed three more times with PBS, resuspended in phenol red-free DMEM, and visualized with an ECHO RVL2-K microscope (USA).

Scratch migration assay

Confluent Huh7.5.1 monolayers were prepared in 6-well plates using DMEM supplemented with 10% FBS. Each well was scratched down the center with a P1000 tip, after which the medium was promptly exchanged for serum-free DMEM with zinc gluconate, $ZnSO_4$, or no supplement (blank). Brightfield images of the identical region of interest (ROI) were captured with an inverted microscope (Novel Optics, Nanjing, China) at 1, 2, and 3 days post-scratch to monitor the leading edge. Migration distance was determined in ImageJ (RRID: SCR_003070) for each time point.

Measurement of intracellular ROS

Intracellular ROS levels were assessed with 2',7'-dichlorodihydrofluorescein diacetate (DCFH-DA). Huh7.5.1 cells were exposed to zinc gluconate or $ZnSO_4$ for 17 h, rinsed with PBS, and stained for 20 min at 37 °C using the DCFH-DA working solution supplied in a ROS detection kit (RRID: AB_2574932, S0034S, Beyotime, Shanghai, China). After PBS washes, the cells were maintained in DMEM without phenol red. 2',7'-dichlorofluorescein (DCF) fluorescence was captured at 488 nm excitation on an ECHO RVL2-K microscope (USA).

Human sphingomyelinase-linked immunoassay

Huh7.5.1 cultures were exposed to zinc gluconate or $ZnSO_4$ for 17 h and then rinsed with PBS (pH 7.2-7.4). The cells were scraped into PBS and lysed by repeated freeze-thaw cycles; after centrifugation at 3,000 rpm for 20 min, the supernatant was collected. Aliquots were transferred to the assay wells, sealed with film, and kept at 37 °C for 60 min. Following five wash steps and blotting dry on clean absorbent paper, 100 μL of 3,3',5,5'-tetramethylbenzidine (TMB) color developer from the sphingomyelinase enzyme-linked immunosorbent assay (SPH-ELISA) detection kit (A101756-48T, Fusheng Industrial, Shanghai, China) was applied, and the plates were held at 37 °C for 15 min. Stop solution (50 μL) was then added to each sample, and absorbance at 450 nm was recorded on a Multiskan GO microplate reader (Thermo Fisher, USA).

Animal administration, blood smear preparation, and platelet enumeration

All animal work was approved by the Animal Ethics Committee of Shandong First Medical University (Approval No. W202504160624). Eight-week-old male BALB/c mice (RRID: MGI:2161072) were obtained from Jinan Pengyue Experimental Animal Breeding (Shandong, China) and housed under specific pathogen-free (SPF) conditions at 23 ± 1 °C with 60 ± 10% relative humidity. After one week of acclimation, the animals were allocated randomly to three groups. Migrasome counting was performed in 11 mice per group, and platelet counting and bleeding volume measurements were performed in 6 mice per group. At baseline, a 20-μL aliquot of diluted tail blood was combined with 380 μL platelet diluent (R20341, Shanghai Yuanye Bio-Technology, Shanghai, China), and platelets were enumerated in a hemocytometer. Tail blood (3-5 μL) was also used to prepare blood films, which were fixed in methanol for 10 min and then stained with Wright's solution for 10 min (C0135, Beyotime, Shanghai, China). Zinc gluconate or $ZnSO_4$ (17 μmol/kg in saline) was then administered by the intraperitoneal route. 24 h later, tail-tip blood was sampled; platelet counts and stained blood films were obtained as at baseline.

Isolation of migrasomes from murine whole blood

Male BALB/c mice (n = 11 per group), eight weeks old, were given an intraperitoneal dose of zinc gluconate (17 μmol/kg), $ZnSO_4$ (17 μmol/kg), or physiological saline. After 24 h under SPF conditions at 23 ± 1 °C, whole blood was drawn. Migrasomes were then purified using the Migralso™ Pro Mouse Immune Cells extraction kit (MGS-P007-MS, Migrasome Therapeutics, Beijing, China). The purified migrasomes were resuspended in PBS, stained with 2 μg/mL WGA for 30 min, and spread evenly onto bovine serum albumin (BSA)-precoated slides for imaging.

Tail transection bleeding test

After isoflurane anesthesia, mice (n = 6 per group) were placed on a flat surface. The distal 5 mm of each tail was amputated. Within 2 min, blood was collected into a capillary tube (10-20 μL; Laixu, Shandong, China) that had been precoated with ethylenediaminetetraacetic acid (EDTA) (ST063, Beyotime, Shanghai, China). The severed tail was then transferred to 50 μL of warm PBS containing 40 mM EDTA and allowed to bleed for 20 min. Finally, the residual blood suspension was placed on a transparent plastic sheet and photographed for documentation.

RNA sequencing

RNA sequencing (RNA-seq) was performed with three biological replicates per group. TRIzol (Invitrogen) was used for total RNA extraction. Sequencing and bioinformatic analysis were carried out by BGI Genomics (Beijing, China), and RNA quality was checked on an Agilent 2100 Bioanalyzer (RRID: SCR_018043). Sequencing used the DNBSEQ platform (RRID: SCR_025899) in PE150 mode. Differentially expressed genes (DEGs) were identified, and Kyoto Encyclopedia of Genes and Genomes (KEGG) pathway and Gene Ontology (GO) enrichment analyses were conducted on the BGI Dr. Tom platform. Figures were prepared with GraphPad Prism 9 (RRID: SCR_002798; GraphPad Software, Inc., La Jolla, CA, USA). The dataset has been submitted to the Gene Expression Omnibus (GEO) (RRID: SCR_005012) and assigned accession number GSE319187.

Data quantification and statistical methods

Fluorescence intensity was quantified in ImageJ. Adobe Illustrator (RRID: SCR 010279, Adobe Inc., San Jose, CA, USA) was used for figure preparation. Statistical testing was carried out in GraphPad Prism 8 (RRID: SCR_002798, GraphPad Software, Inc., La Jolla, CA, USA). Paired t-tests were applied to platelet count data. Comparisons involving two groups were made with unpaired two-tailed t-tests. When more than two groups were compared, one-way analysis of variance (ANOVA) was used, followed by Tukey-Kramer post hoc testing. Values are presented as mean ± standard error of the mean (SEM). Symbols indicate significance as follows: not significant (NS), $P > 0.05$; $^{*}P < 0.05$; $^{**}P < 0.01$; $^{***}P < 0.001$; $^{****}P < 0.0001$.

RESULTS

Physiological zinc concentrations inhibit migrasome formation

Zinc is an indispensable trace metal for humans that participates in diverse cellular processes and helps maintain ionic balance, with normal blood concentrations of 8-23 μM[17]. $ZnSO_4$ and zinc gluconate are commonly used zinc supplements[18]. Before evaluating their effects on migrasome formation, we exposed Huh7.5.1 cells to 0-30 μM $ZnSO_4$ or zinc gluconate for 24 h and assessed viability with a CCK-8 assay. Cell viability was unaffected across this range [Figure 1A and B].

We then used WGA, a migrasome marker[19], to stain Huh7.5.1 cells and examine how zinc concentration affects migrasome formation. Zinc ions inhibited migrasome formation at 10-30 μM [Figure 1C and D], and retraction fiber extension was also suppressed at 10 and 30 μM. At 20 μM, retraction fibers were reduced, though the difference was not statistically significant [Figure 1C and E].

To confirm intracellular zinc ions accumulation, we used TSQ staining. After 17 h treatment with 20 μmol/L zinc gluconate, migrasome numbers were significantly lower than in untreated cells [Figure 1F and G], and TSQ fluorescence showed much higher intracellular zinc ions levels in zinc gluconate-treated cells than in controls [Figure 1F and H]. Similar results were obtained with 20 μmol/L $ZnSO_4$ [Figure 1I-K]. In scratch assays, cell migration was also inhibited in Huh7.5.1 cells treated with zinc gluconate or $ZnSO_4$ [Supplementary Figure 1A and B]. These data suggest that zinc ions alter cell migration dynamics, as summarized in the schematic [Figure 1L].

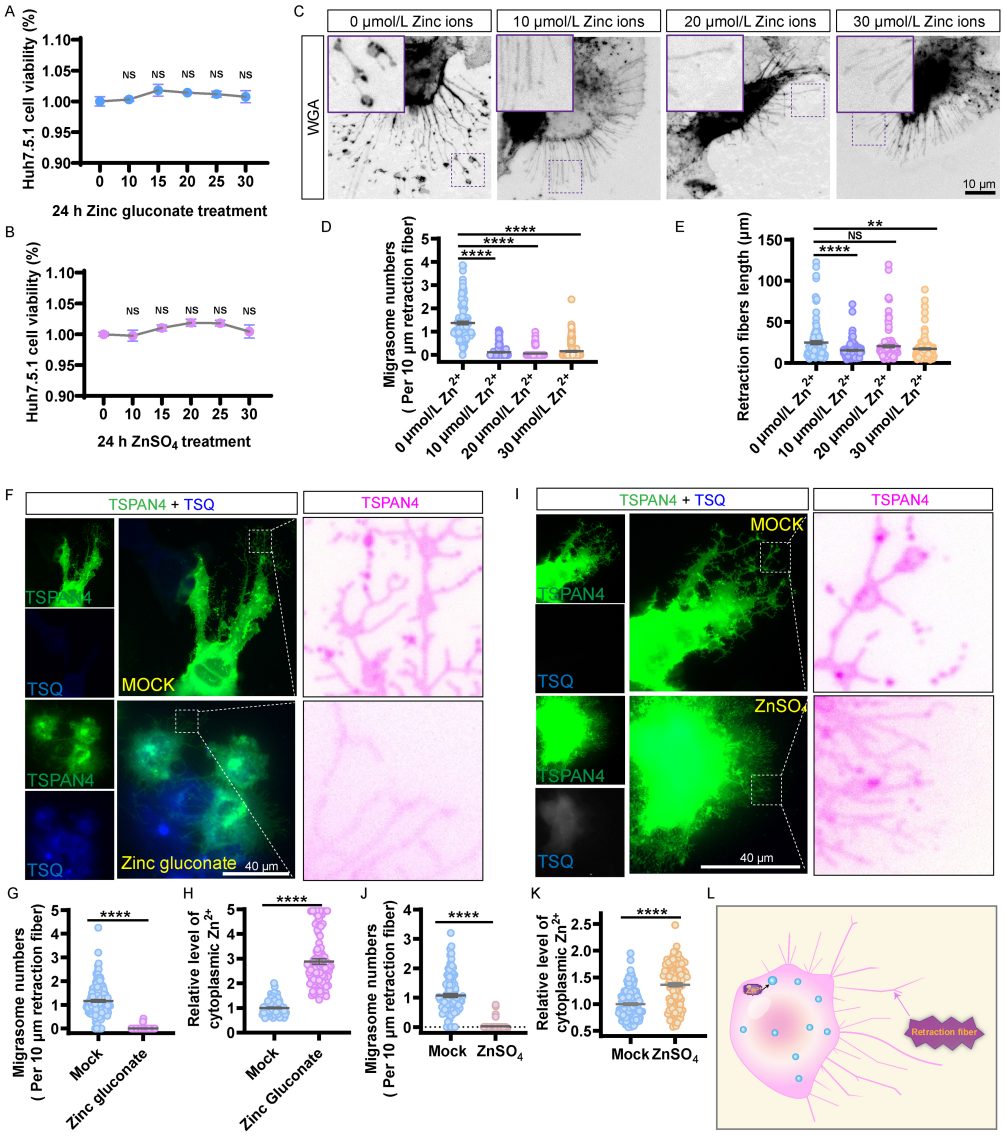


Figure 1. Zinc ions inhibit migrasome formation. (A) Viability of Huh7.5.1 cells exposed to increasing concentrations of zinc gluconate (0-30 μmol/L) for 24 h, as evaluated by the CCK-8 viability assay. Values are derived from five independent experiments; (B) Viability of Huh7.5.1 cells exposed to increasing concentrations of $ZnSO_4$ (0-30 μmol/L) for 24 h, as evaluated by the CCK-8 viability assay; (C) Photomicrographs of Huh7.5.1 cells stained with WGA following treatment with varying concentrations of zinc ions (0 to 30 μmol/L) for 17 h. Scale bar: 10 μm; (D and E) Statistical data from (C) include migrasome counts per 10 μm retraction fibers (D) and the lengths of retraction fibers (E). For each group, at least 107 cells were analyzed across three independent experiments; (F) Images of eGFP-TSPAN4-expressing Huh7.5.1 cells incubated with 20 μmol/L zinc gluconate for 17 h and stained with TSQ as a zinc ion marker. A magnified view highlights the migrasomes and retraction fibers in eGFP-TSPAN4-expressing Huh7.5.1 cells. Scale bar: 40 μm; (G) Statistical data from (F) include migrasome counts per 10 μm retraction fibers. For each group, at least 116 cells were analyzed across three independent experiments; (H) Statistical analyses of relative level of cytoplasmic zinc in (F). For each group, at least 103 cells were analyzed across three independent experiments; (I) Images of Huh7.5.1 cells expressing eGFP-TSPAN4 incubated with 20 μmol/L $ZnSO_4$ for 17 h and stained with TSQ as a zinc ion marker. A magnified view illustrates the migrasomes and retraction fibers in Huh7.5.1 cells expressing eGFP-TSPAN4. Scale bar: 40 μm; (J) Statistical analyses of migrasome counts per 10 μm retraction fibers in (I). For each group, at least 104 cells were analyzed across three independent experiments; (K) Statistical analyses of relative level of cytoplasmic zinc in (I). For each group, at least 113 cells were analyzed across three independent experiments. Data are shown as mean ± SEM. NS denotes $P > 0.05$; $^{*}P < 0.05$; $^{**}P < 0.01$; $^{***}P < 0.001$; $^{****}P < 0.0001$. (L) Diagram showing zinc ions inhibit migrasome formation. CCK-8: Cell counting Kit-8; eGFP: enhanced green fluorescent protein; NS: not significant; SEM: standard error of the mean; TSPAN4: tetraspanin 4; TSQ: N-(6-methoxy-8-quinolyl)-p-toluenesulfonamide; WGA: wheat germ agglutinin.

Forced zinc ions export reverses the inhibition of migrasome formation

Disulfiram enhances zinc ions efflux through solute carrier family 30A (SLC30A) transporters[20]. To determine whether the inhibitory effect depends on intracellular zinc ions, we treated Huh7.5.1 cells with disulfiram together with zinc ions supplements. Disulfiram not only increased migrasome numbers on its own but also fully reversed the suppression caused by zinc gluconate [Figure 2A and B]; at the same time, the zinc ions concentration in cytoplasmic was reduced in disulfiram treated cells [Figure 2A and C]. A similar reversal was observed in cells treated with 20 μmol/L $ZnSO_4$ [Figure 2D-F]. At 17 h, the zinc ions concentration in the culture medium of cells treated with disulfiram plus zinc ions was far higher than that in the medium of cells treated with zinc ions alone [Figure 2G]. A schematic representation of disulfiram-mediated zinc ions efflux is shown in Figure 2H.

Blocking extracellular zinc ions uptake reverses zinc ions-induced inhibition of migrasome formation

Zinc transport between intracellular and extracellular compartments is mediated by the solute carrier family 39A (SLC39A) and SLC30A families[21]. To prevent extracellular zinc ions from entering cells, we used an antibody against SLC39A6, which competitively blocks zinc ions uptake. Anti-SLC39A6 treatment alone increased migrasome numbers and completely reversed the inhibitory effect of zinc gluconate [Figure 3A and B]. Cytoplasmic zinc ions levels were lower in anti-SLC39A6-treated cells [Figure 3A and C]. The same effect was observed with $ZnSO_4$ [Figure 3D-F]. After 17 h, zinc ions concentration in the culture medium of cells treated with anti-SLC39A6 plus zinc was much higher than that of cells treated with zinc ions alone [Figure 3G]. The proposed mechanism of antibody-mediated blockade is illustrated in Figure 3H.

Zinc ions supplementation reduces migrasome numbers and impairs platelet function in mice

To test whether $ZnSO_4$ affects migrasome numbers *in vivo*, mice were injected intraperitoneally once with $ZnSO_4$ (17 μmol/kg) or saline, and whole-blood migrasomes were isolated 24 h later [Figure 4A]. $ZnSO_4$ treatment significantly reduced circulating migrasome counts relative to saline controls [Figure 4B and C]. Next, we assessed platelet parameters. Blood collected 24 h after injection showed significant decreases in platelet count [Figure 4D] and platelet aggregation [Figure 4E], along with increased bleeding volumes [Figure 4F-H]. As migrasomes have been reported to promote platelet release from neutrophils and to influence platelet counts and function [Figure 4I][15], these results suggest that $ZnSO_4$ impairs platelet production and activation, potentially compromising hemostatic function.

We then tested zinc gluconate under similar conditions. Intraperitoneal injection of 17 μmol/kg zinc gluconate also reduced whole-blood migrasome numbers [Figure 5A and B] and led to lower platelet counts [Figure 5C] and aggregation [Figure 5D], with increased bleeding volume [Figure 5E-G]. Together, these results show that both zinc ions supplements reduce migrasome availability and impair platelet function, thereby potentially affecting hemostasis [Figure 5H].

Physiological zinc ions concentrations suppress cholesterol level

Next, we examined the transcriptional response to $ZnSO_4$ and zinc gluconate. RNA-seq of Huh7.5.1 cells incubated with 20 μmol/L of each compound identified 2,693 up-regulated and 2,590 down-regulated genes in $ZnSO_4$-treated cells relative to controls [Supplementary Figure 2A], and 3,000 up-regulated and 2,846 down-regulated genes in zinc gluconate-treated cells [Supplementary Figure 2B]. Both treatments shared 4,826 regulated genes [Supplementary Figure 2C]. GO and KEGG enrichment analyses revealed significant changes in lipid metabolism [Figure 6A], with most cholesterol metabolism genes down-regulated [Figure 6B] and most cholesterol synthase genes up-regulated [Figure 6C]. Filipin staining confirmed that both zinc ions treatments markedly reduced plasma membrane cholesterol levels after 17 h compared with untreated controls [Figure 6D-G].

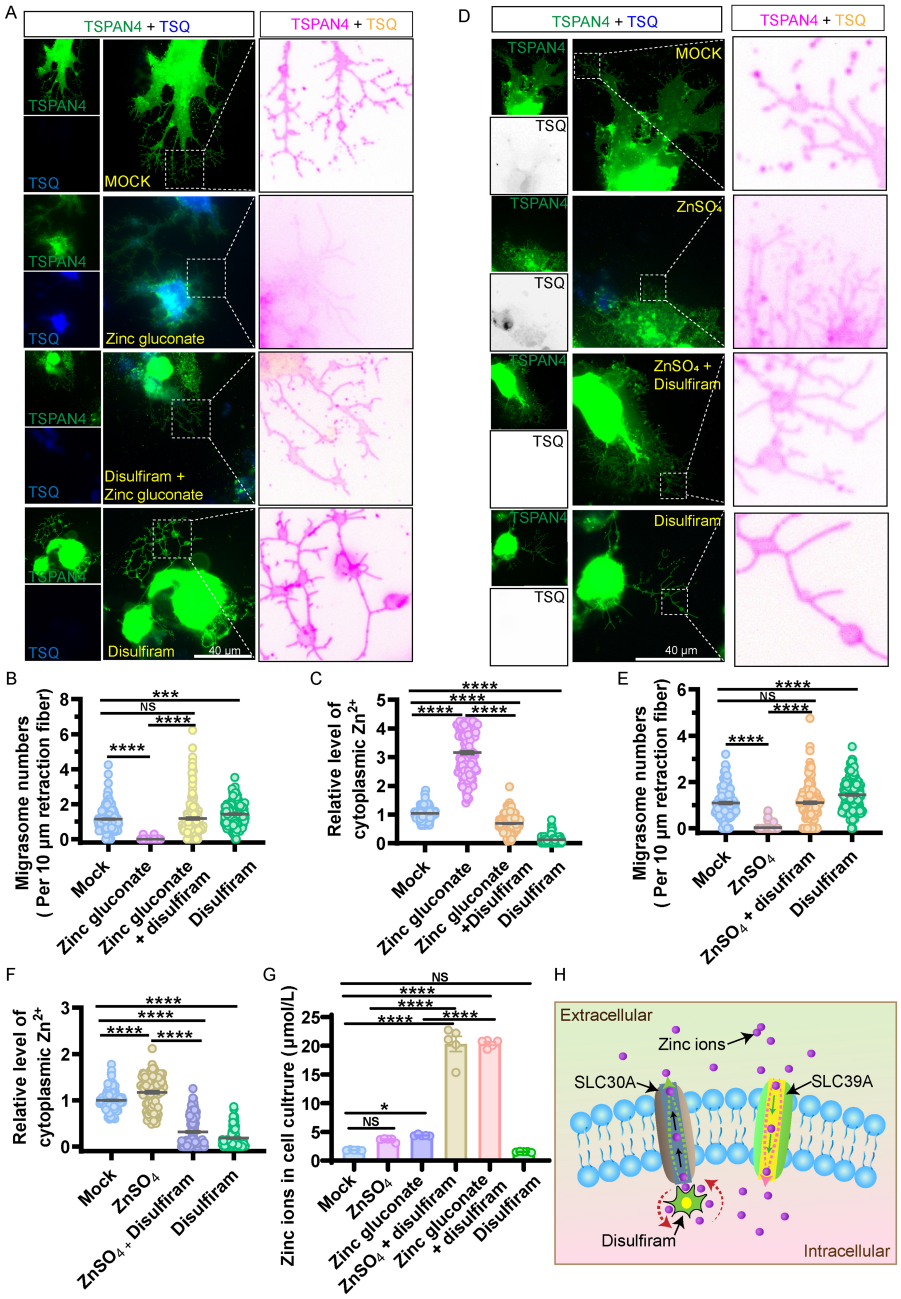


Figure 2. Removal of intracellular zinc ions can reverse the inhibition of migrasome biogenesis induced by zinc ions. (A) Images of eGFP-TSPAN4-expressing Huh7.5.1 cells incubated with 20 μmol/L zinc gluconate, 5 μmol/L disulfiram (which can pump zinc ions out of the cells), zinc gluconate with disulfiram, or a mock treatment for 17 h and stained with TSQ for zinc. Scale bar: 40 μm; (B) Statistical analyses of migrasome counts per 10 μm retraction fibers in (A). For each group, at least 122 cells were analyzed across three independent experiments; (C) Statistical analyses of relative level of cytoplasmic zinc in (A). For each group, at least 135 cells were analyzed across three independent experiments; (D) Images of eGFP-TSPAN4-expressing Huh7.5.1 cells incubated with 20 μmol/L $ZnSO_4$, disulfiram, $ZnSO_4$ with disulfiram, or mock treatment for 17 h and stained with TSQ. Scale bar: 40 μm; (E) Migrasome counts per 10 μm retraction fibers from (D). For each group, at least 111 cells were analyzed across three independent experiments; (F) Statistical analyses of relative level of cytoplasmic zinc in (D). For each group, at least 109 cells were analyzed across three independent experiments; (G) Concentration of zinc ions in the huh7.5.1 cell culture after treatment with 20 μmol/L $ZnSO_4$, 20 μmol/L zinc gluconate, 5 μmol/L disulfiram, $ZnSO_4$ with disulfiram, zinc gluconate with disulfiram and mock for 17 h. Data are shown as mean ± SEM. NS denotes $P > 0.05$; ***$P < 0.001$; ****$P < 0.0001$; (H) Diagram of disulfiram's role in expelling intracellular zinc ions to the extracellular space. eGFP: Enhanced green fluorescent protein; NS: not significant; SEM: standard error of the mean; SLC30A: solute carrier family 30A; SLC39A: solute carrier family 39A; TSPAN4: tetraspanin 4; TSQ: N-(6-methoxy-8-quinolyl)-p-toluenesulfonamide.

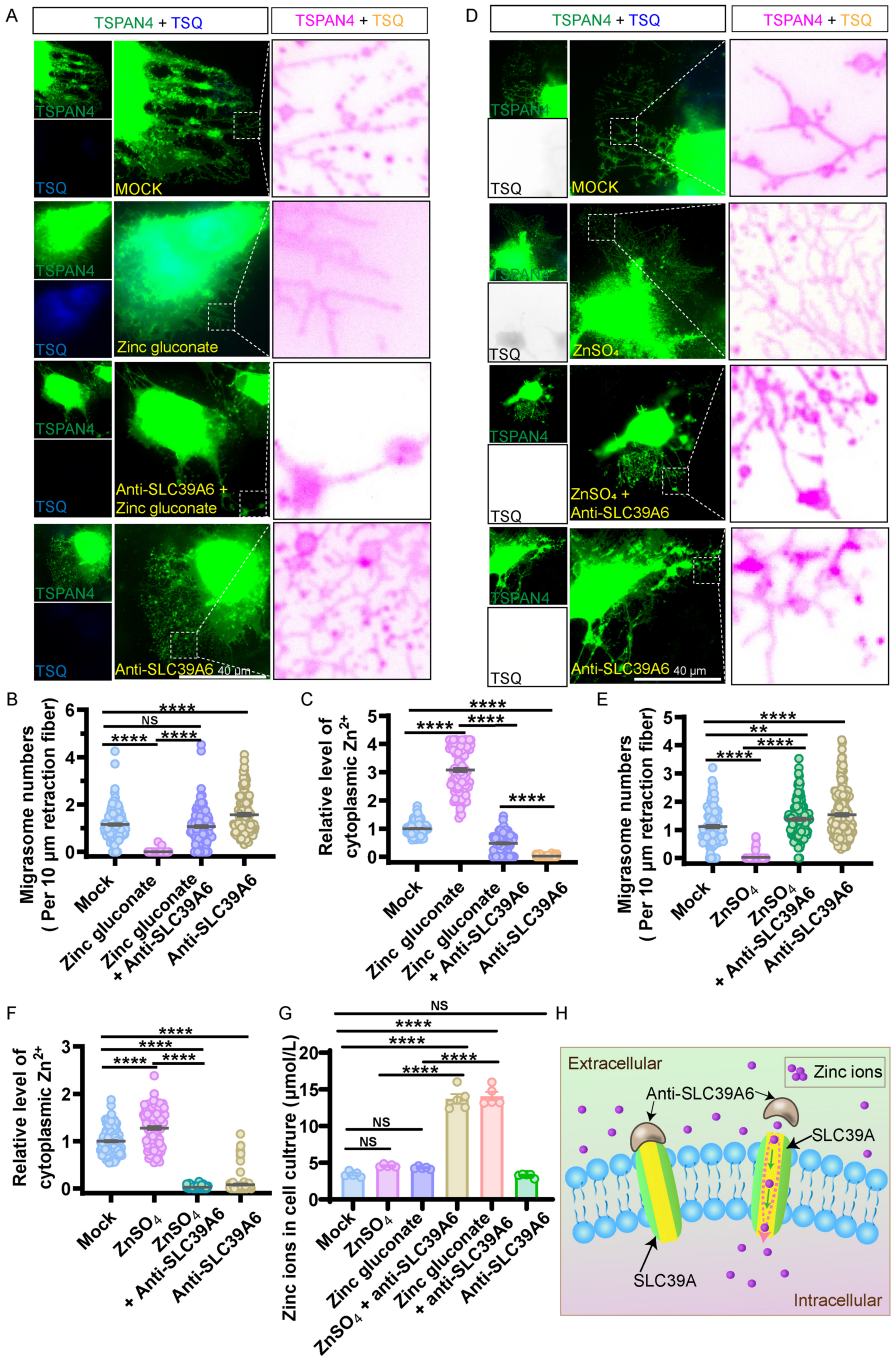


Figure 3. Preventing extracellular zinc ions entry can reverse migrasome inhibition. (A) Images of eGFP-TSPAN4-expressing Huh7.5.1 cells incubated with 20 μmol/L zinc gluconate, 10 ng/mL Anti-SLC39A6 (which inhibits zinc ion entry into cells), zinc gluconate with Anti-SLC39A6, or a mock treatment for 17 h and stained with TSQ for zinc ions. Scale bar: 40 μm; (B) Migrasome counts per 10 μm retraction fibers in (A). For each group, at least 123 cells were analyzed across three independent experiments; (C) Statistical analyses of relative level of cytoplasmic zinc ions in (A). For each group, at least 85 cells were analyzed across three independent experiments; (D) Images of eGFP-TSPAN4-expressing Huh7.5.1 cells incubated with 20 μmol/L $ZnSO_4$, 10 ng/mL Anti-SLC39A6, $ZnSO_4$ with Anti-SLC39A6, or mock treatment for 17 h and stained with TSQ for zinc ions. Scale bar: 40 μm; (E) Migrasome counts per 10 μm retraction fibers in (D). For each group, at least 108 cells were analyzed across three independent experiments; (F) Statistical analyses of relative level of cytoplasmic zinc ions in (D). For each group, at least 106 cells were analyzed across three independent experiments; (G) Concentration of zinc ions in the huh7.5.1 cell culture after treatment with 20 μmol/L $ZnSO_4$, 20 μmol/L zinc gluconate, 10 ng/mL Anti-SLC39A6, $ZnSO_4$ with Anti-SLC39A6, zinc gluconate with Anti-SLC39A6 and mock for 17 h. Data are shown as mean ± SEM. NS denotes $P > 0.05$; $^{**}P < 0.01$; $^{***}P < 0.001$; $^{****}P < 0.0001$; (H) Schematic diagram illustrating how Anti-SLC39A6 blocks zinc ions entry into cells. eGFP: Enhanced green fluorescent protein; NS: not significant; SEM: standard error of the mean; SLC39A: solute carrier family 39A; SLC39A6: solute carrier family 39 member 6; TSPAN4: tetraspanin 4; TSQ: N-(6-methoxy-8-quinolyl)-p-toluenesulfonamide.

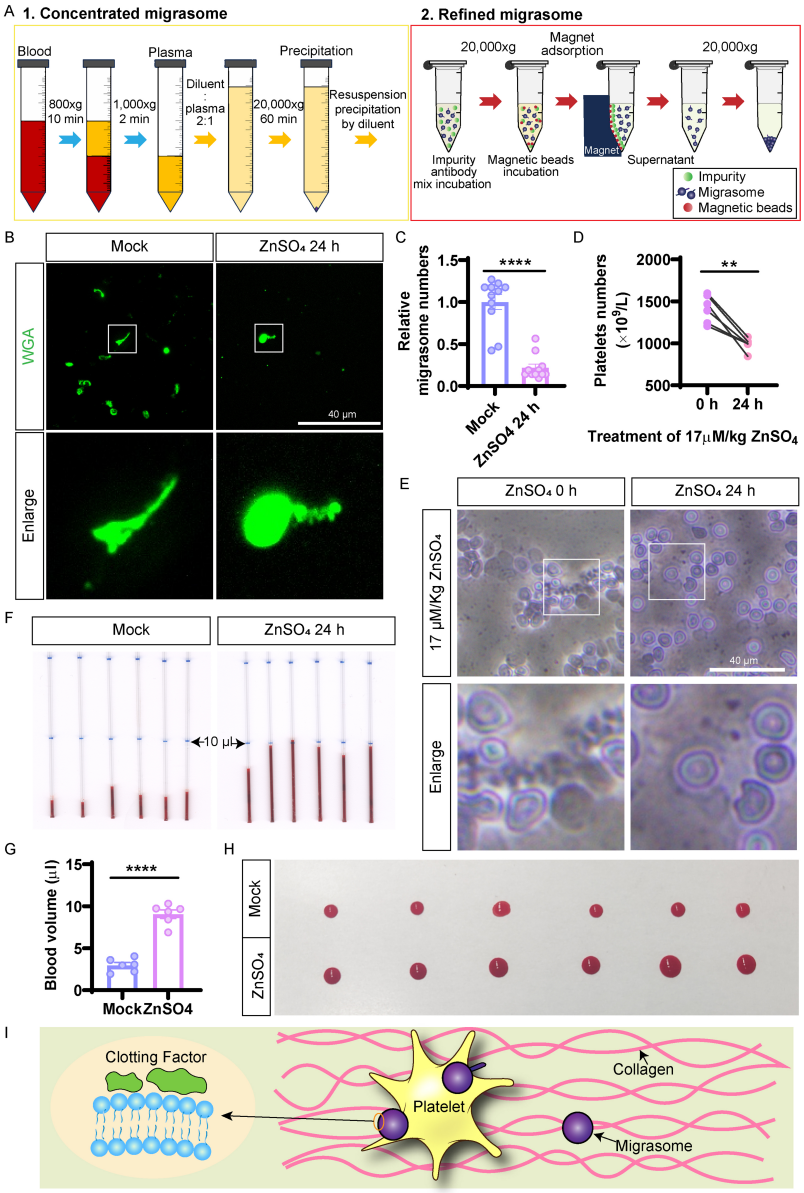


Figure 4. Effects of $ZnSO_4$ on migrasomes and platelet dynamics in mice. (A) Schematic overview of the migrasome isolation workflow from mouse blood. In step 1, crude migrasomes are collected by concentration. In step 2, migrasomes are further purified with the Migralso™ Pro Mouse Immune Cell Extraction Kit; (B) $ZnSO_4$ treatment inhibited migrasome formation in mouse blood. Scale bar: 40 μm; (C) Statistical evaluation of the data in (B) (n = 11 mice per group); (D) Platelet counts in mouse blood at 0 and 24 h after $ZnSO_4$ treatment were statistically analyzed (n = 6 mice per group); (E) Representative images of platelet aggregates in blood smears from $ZnSO_4$-treated mice. Scale bar: 40 μm; (F) Assessment of peripheral vascular bleeding in mice after 24 h of $ZnSO_4$ treatment (n = 6 mice per group); (G) Statistical analysis of the results in (F); (H) Peripheral vascular bleeding was compared between mice incubated with $ZnSO_4$ for 24 h and untreated controls (n = 6 mice per group). Data are shown as mean ± SEM. $^{**}P < 0.01$; $^{****}P < 0.0001$; (I) Schematic showing how blood migrasomes affect platelet function and coagulation dynamics. SEM: Standard error of the mean; WGA: wheat germ agglutinin.

To determine whether cholesterol replenishment could reverse this inhibition, 25 μmol/L cholesterol was added to cells exposed to zinc ions. Cholesterol supplementation significantly increased migrasome numbers compared with zinc ions-treated controls [Figure 6H and I], and retraction fibers tended to lengthen, though this change was less pronounced [Figure 6H and J]. These results indicate that cholesterol availability is critical for counteracting zinc ions-induced suppression of migrasome formation [Figure 6K].

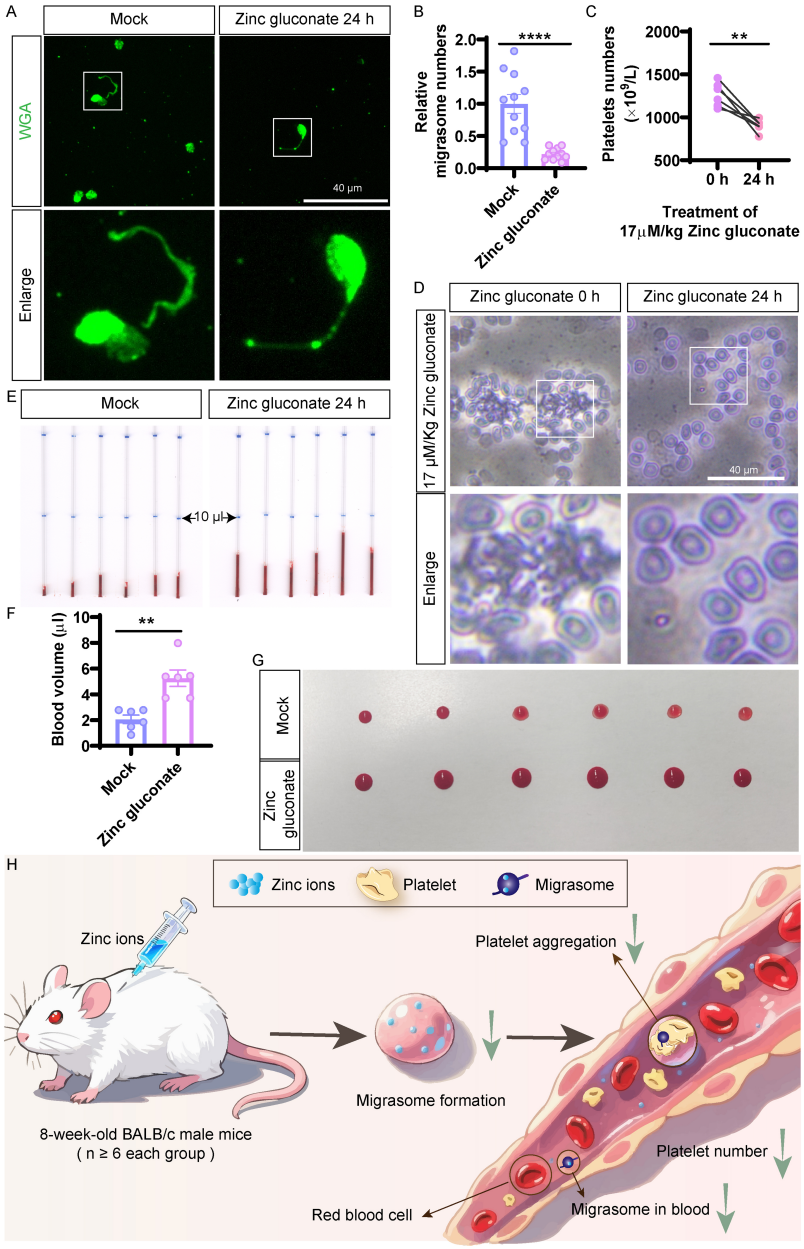


Figure 5. Effects of zinc gluconate on migrasomes and platelet dynamics in mice. (A) Zinc gluconate treatment inhibited migrasome formation in mouse blood. Scale bar: 40 μm; (B) Statistical analysis based on (A) (n = 11 mice per group); (C) Platelet counts in mouse blood before and 24 h after zinc gluconate treatment were statistically evaluated (n = 6 mice per group); (D) Images representative of aggregated platelets in blood smears from zinc gluconate-treated mice. Scale bar: 40 μm; (E) Evaluation of peripheral vascular bleeding after 24 h of zinc gluconate treatment in mice (n = 6 mice per group); (F) Statistical analysis of the data in (E); (G) Peripheral vascular bleeding in mice after 24 h of zinc gluconate treatment *vs*. untreated controls (n = 6 mice per group). Values are mean ± SEM. $^{**}P < 0.01$; $^{****}P < 0.0001$; (H) Diagram illustrating the effect of reduced migrasome levels on blood clotting. SEM: Standard error of the mean.

Effects of zinc ions on sphingomyelin, phosphatidylinositol-4,5-bisphosphate (PI(4,5)P_2), guanosine triphosphate (GTP)-bound Ras homolog family member A (RhoA), and ROS levels

Sphingomyelin is critical for migrasome formation, and previous studies show that zinc ions reduce sphingomyelin levels[22]. In zinc ions-treated cells, we observed downregulation of SGMS1, SPTLC1, SPTLC3, CERS1, CERS2, and NFKBIA, genes associated with sphingomyelin activity [Figure 7A]. Both $ZnSO_4$ and zinc gluconate reduced sphingomyelin levels [Figure 7B]. To test whether sphingomyelin depletion mediates zinc ions-induced inhibition, we supplemented zinc ions-treated Huh7.5.1 cells with sphingomyelin. Cells

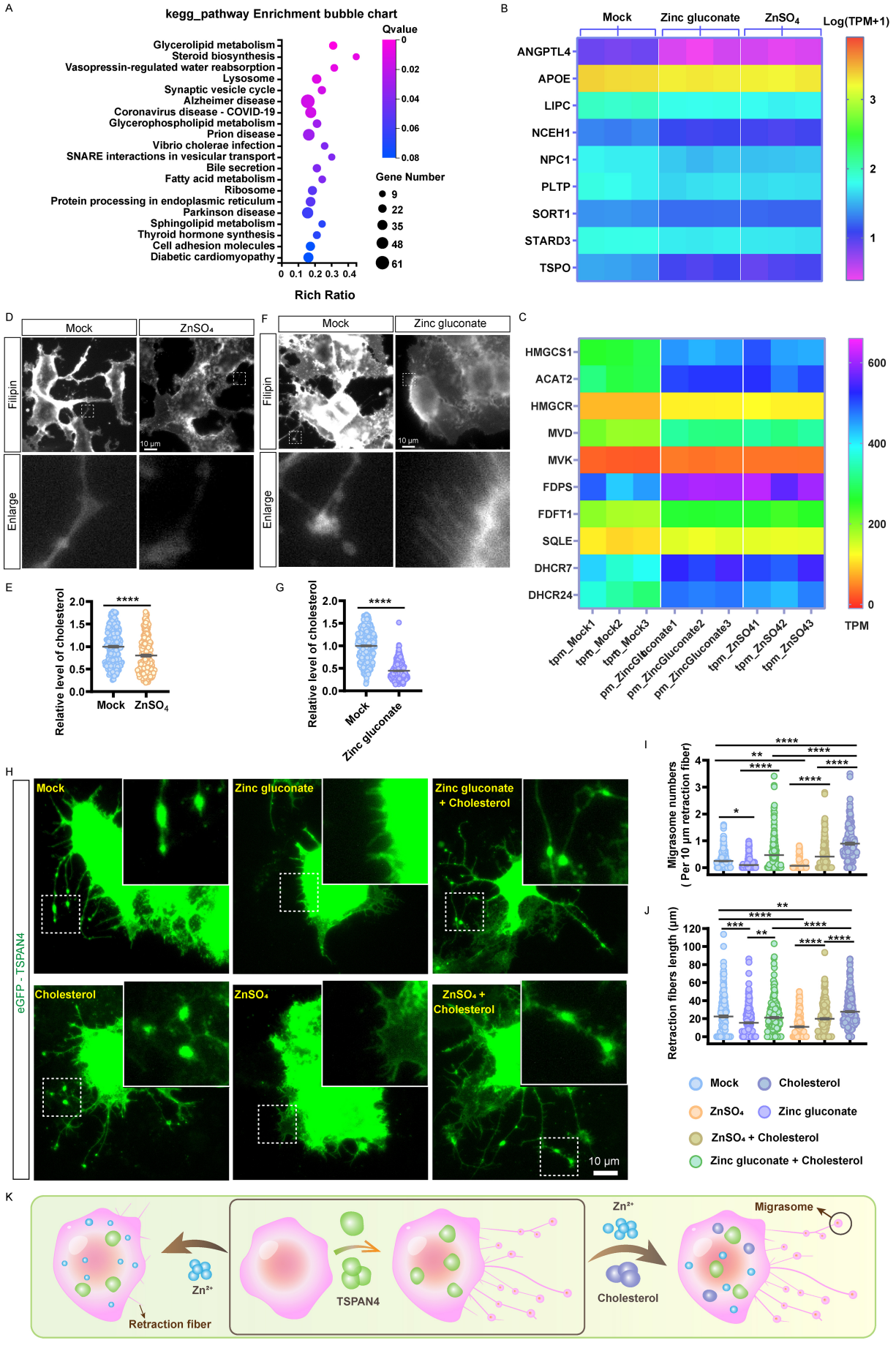


Figure 6. Zinc ions reduce cholesterol level. (A) RNA sequencing analysis was carried out on DEGs identified in both the zinc gluconate

and $ZnSO_4$ models, then subjected to KEGG enrichment analysis of pathways associated with lipid metabolism; (B) Expression levels of gene clusters associated with cholesterol metabolism; (C) Expression of gene clusters associated with cholesterol synthase; (D) Huh7.5.1 cells incubated with 20 μmol/L $ZnSO_4$ for 17 h were labeled with filipin. Scale bar: 10 μm; (E) Statistical analysis of relative membrane cholesterol levels in $ZnSO_4$-treated cells. For each group, at least 220 cells were analyzed across three independent experiments; (F) Huh7.5.1 cells incubated with 20 μmol/L zinc gluconate for 17 h. were labeled with filipin. Scale bar: 10 μm; (G) Statistical analysis of relative membrane cholesterol levels in zinc gluconate-treated cells. For each group, at least 255 cells were analyzed across three independent experiments; (H) Images of eGFP-TSPAN4-expressing Huh7.5.1 cells incubated with 20 μmol/L zinc gluconate, 20 μmol/L $ZnSO_4$, zinc gluconate with cholesterol, $ZnSO_4$ with cholesterol, and 25 μmol/L cholesterol for 17 h. Scale bar: 10 μm; (I) Statistical analyses of migrasome counts per 10 μm retraction fibers in (H); (J) Statistical analyses of retraction fiber lengths in (H). For each group, at least 206 cells were analyzed across three independent experiments. Data are shown as mean ± SEM. $^{**}P < 0.01$; $^{***}P < 0.001$; $^{****}P < 0.0001$; (K) Zinc ions inhibit migrasome formation, whereas cholesterol supplementation partially restores it. DEGs: Differentially expressed genes; eGFP: enhanced green fluorescent protein; HMGCR: 3-hydroxy-3-methylglutaryl-CoA reductase; KEGG: Kyoto Encyclopedia of Genes and Genomes; SEM: standard error of the mean; TSPAN4: tetraspanin 4; TPM: transcripts per million.

supplemented with 10 μmol/L sphingomyelin after zinc ions treatment showed a significant increase in migrasome numbers compared with zinc ions-treated cells [Figure 7C and D], and retraction fibers showed a similar but weaker trend [Figure 7C and E]. These results suggest that zinc ions-induced sphingomyelin reduction inhibits migrasome formation, and sphingomyelin supplementation promotes migrasome development [Figure 7F].

PI(4,5)P2 is also critical for migrasome biogenesis[23,24]. To examine whether zinc affects PI(4,5)P2 levels, we transfected Huh7.5.1 cells with PH-PLCD1-GFP, a PI(4,5)P2 probe. After 17 h exposure to 20 μM $ZnSO_4$ or zinc gluconate, immunofluorescence showed no significant change in PH-PLCD1 signal [Figure 7G-J].

Signaling through RhoA and its downstream effector Rho-associated protein kinase 1 (ROCK1)[25]. RNA-seq suggested that actin cytoskeleton and focal adhesion pathways regulate RhoA GTP activity [Supplementary Figure 2D]. To test this possibility, Huh7.5.1 cells were transfected with eGFP-2×-Rhotekin-GBD, a probe for GTP-bound RhoA. Immunofluorescence analysis after treatment revealed increased signal in cells treated with zinc gluconate [Figure 7K and L], but no significant change in $ZnSO_4$-treated cells [Figure 7M and N].

RNA-seq also indicated changes in autophagy, autophagosome, and mechanistic target of rapamycin (mTOR) signaling upon zinc ions treatment [Supplementary Figure 2D and E]. Both $ZnSO_4$ and zinc gluconate reduced intracellular ROS levels and mitigated ROS activation induced by ZnO-NPs [Figure 7O-R].

DISCUSSION

The present work assessed the impact of two zinc supplements, $ZnSO_4$ and zinc gluconate, on migrasome biogenesis, platelet function, and coagulation *in vivo* and explored the underlying molecular mechanisms. Our data show that zinc ions suppress migrasome biogenesis by lowering intracellular levels of cholesterol, sphingomyelin, and ROS, thereby limiting platelet aggregation and, potentially, thrombus formation [Figure 8].

Transcriptomic profiling was performed on Huh7.5.1 cells exposed to 20 μmol/L $ZnSO_4$ or zinc gluconate, revealing significant enrichment of changes in lipid metabolism pathways. Given the dependence of migrasome formation on cholesterol[14], we measured cellular cholesterol content and observed a marked decrease following zinc ions treatment. Data from the National Health and Nutrition Examination Survey (NHANES) have previously linked dietary zinc intake to lower levels of highly sensitive C-reactive protein, triglycerides, and high-density lipoprotein cholesterol[26]. In diabetic patients, zinc supplementation also reduced total cholesterol[27]. However, how zinc ions lower cholesterol levels remains unclear. We therefore measured the activity of 3-hydroxy-3-methylglutaryl-CoA reductase (HMGCR), the rate-limiting enzyme in

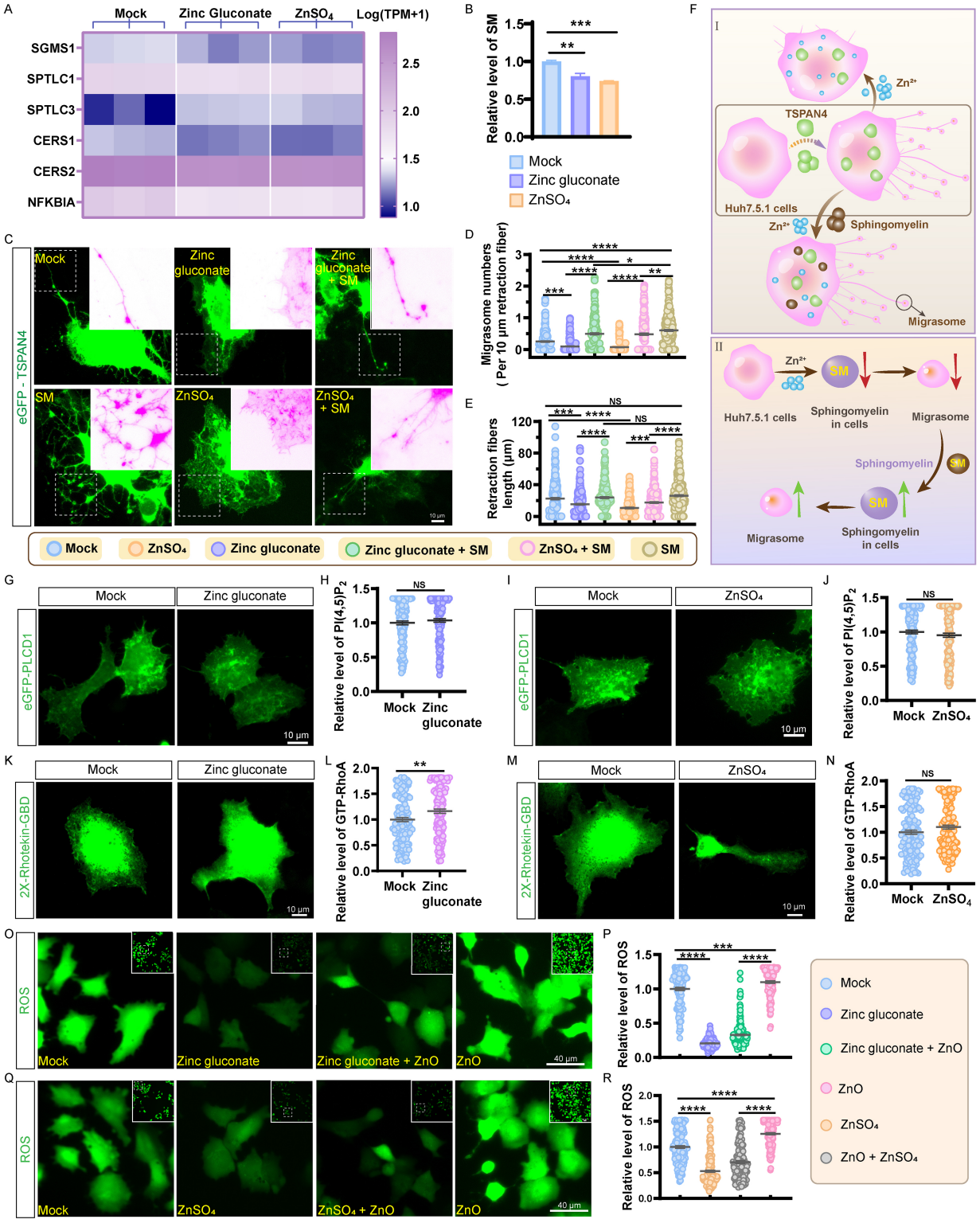


Figure 7. Zinc ions downregulate sphingomyelin levels. (A) Expression levels of gene clusters involved in sphingomyelin metabolism; (B) Relative sphingomyelin levels in Huh7.5.1 cells incubated with 20 μmol/L zinc gluconate and 20 μmol/L $ZnSO_4$ for 17 h. Values are derived from three independent experiments; (C) Images of eGFP-TSPAN4-expressing Huh7.5.1 cells incubated with 20 μmol/L zinc gluconate, 20 μmol/L $ZnSO_4$, zinc gluconate with sphingomyelin, $ZnSO_4$ with sphingomyelin, and 10 μmol/L sphingomyelin for 17 h. Scale bar: 10 μm; (D) Statistical evaluation of migrasome counts per 10 μm retraction fibers is shown in (C). For each group, at least 200 cells were analyzed across three independent experiments; (E) Statistical analyses of retraction fiber lengths in (C). For each group, at least 200 cells were analyzed across three independent experiments; (F) Schematic diagram showing that zinc ions inhibit migrasome formation, and that sphingomyelin replenishment partially reverses this inhibition; (G) Representative images of PH-eGFP-PLCD1-expressing Huh7.5.1 cells were incubated with or without zinc gluconate, and representative images are shown. Scale bar: 10 μm; (H) Statistical analysis of (G). For each group, at least 139 cells were analyzed across three independent experiments; (I) Representative images of PH-eGFP-PLCD1-expressing Huh7.5.1 cells incubated with $ZnSO_4$. Scale bar: 10 μm; (J) Data in (I) were statistically analyzed using more than 166 cells in

every group across three independent experiments; (K) Huh7.5.1 cells expressing eGFP-2X-Rhotekin-GBD incubated with or without zinc gluconate for 17 h. Scale bar: 10 μm; (L) Data in (K) were statistically analyzed using more than 129 cells in every group across three independent experiments; (M) Huh7.5.1 cells expressing eGFP-2X-Rhotekin-GBD incubated with $ZnSO_4$ for 17 h. Scale bar: 10 μm; (N) Data in (M) were statistically analyzed using more than 142 cells in every group across three independent experiments; (O) Huh7.5.1 cells were incubated for 17 h with 20 μmol/L zinc gluconate, 20 μg/mL 30 nm ZnO-NPs, or a combination of zinc gluconate and ZnO-NPs, and then labeled with DCFH-DA to assess ROS levels. Scale bar: 40 μm; (P) Statistical analysis of relative ROS levels in zinc gluconate-treated cells. For each group, at least 117 cells were analyzed across three independent experiments; (Q) Huh7.5.1 cells were incubated for 17 h with 20 μmol/L $ZnSO_4$, 20 μg/mL 30 nm ZnO-NPs, or a combination of $ZnSO_4$ and ZnO-NPs, and then labeled with DCFH-DA to assess ROS levels. Scale bar: 40 μm; (R) Statistical analysis of relative ROS levels in $ZnSO_4$-treated cells. For each group, at least 132 cells were analyzed across three independent experiments. Data are shown as mean ± SEM. NS denotes $P > 0.05$; $^{*}P < 0.05$; $^{**}P < 0.01$; $^{***}P < 0.001$; $^{****}P < 0.0001$. DCF: 2′,7′-dichlorofluorescein; DCFH-DA: 2′,7′-dichlorodihydrofluorescein diacetate; eGFP: enhanced green fluorescent protein; GBD: GTPase-binding domain; GFP: green fluorescent protein; NS: not significant; PH: pleckstrin homology domain; PI(4,5)P2: phosphatidylinositol 4,5-bisphosphate; PLCD1: phospholipase C delta 1; RhoA: Ras homolog family member A; ROS: reactive oxygen species; SEM: standard error of the mean; SM: sphingomyelin; TPM: transcripts per million; TSPAN4: tetraspanin 4; ZnO: zinc oxide; ZnO-NPs: zinc oxide nanoparticles.

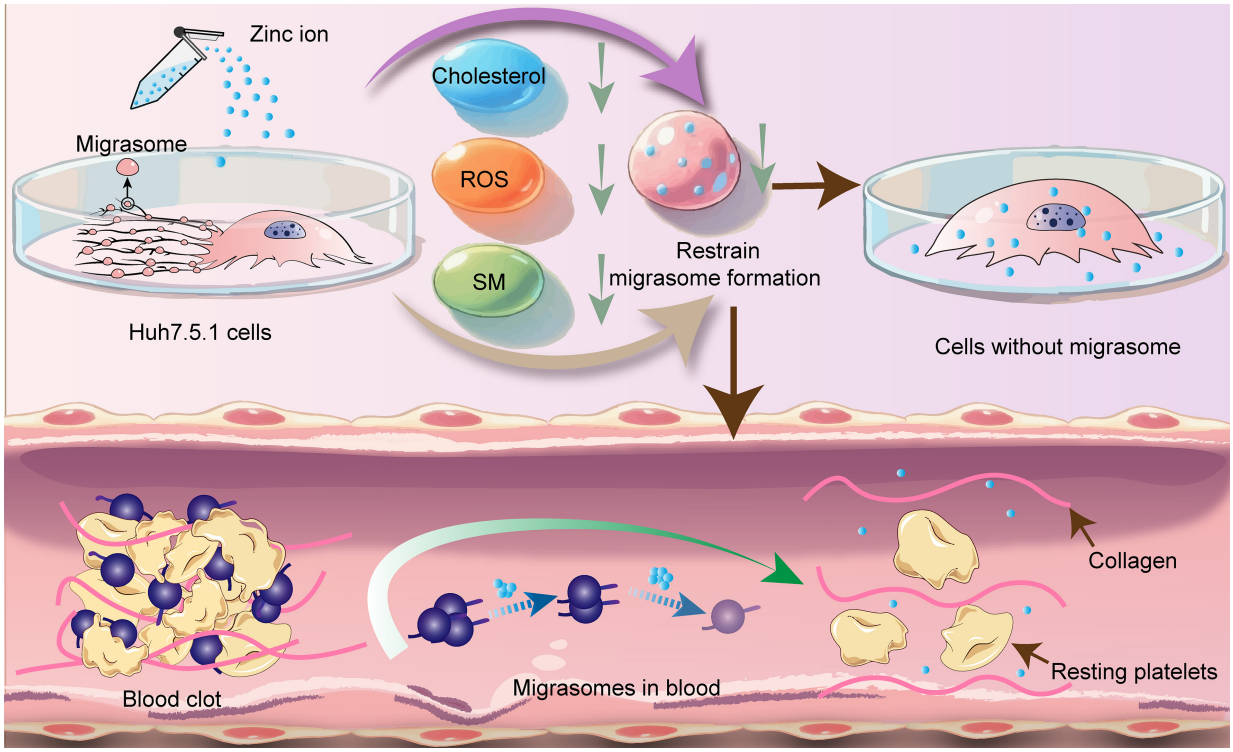


Figure 8. Model depicting the role of zinc ions in migrasome formation. All graphical elements are original, and no third-party copyrighted material was used. ROS: Reactive oxygen species; SM: sphingomyelin.

cholesterol synthesis. Surprisingly, zinc ions significantly increased HMGCR activity [Supplementary Figure 3]. This is consistent with zinc interfering with the efficacy of statins[28], which inhibit HMGCR activity[29]. Although our RNA-seq analysis revealed transcriptomic changes in autophagy, autophagosome, and mTOR signaling after zinc ions treatment, we focused our mechanistic model on cholesterol and sphingomyelin biosynthesis. This choice was guided by functional rescue experiments: supplementation with cholesterol or sphingomyelin partially restored migrasome formation in zinc ions-treated cells, providing causal evidence that these metabolic pathways directly contribute to migrasome biogenesis. In contrast, the changes in mTOR/autophagy-related genes may represent secondary or parallel responses to zinc ions-induced ROS reduction, rather than the primary driver of migrasome inhibition.

We previously reported that ZnO-NPs promote migrasome formation[16], whereas the present work shows that soluble zinc ions exert an opposite effect. This contrast suggests that whether zinc exists as free ions or

solid compounds determines its influence on migrasome dynamics, probably through different routes of cellular entry and downstream signaling.

Earlier studies proposed that low concentrations of zinc ions inhibit platelet aggregation via the prostaglandin I_2 (PGI_2) pathway[30]. However, our transcriptomic data did not detect significant changes in PGI_2 synthase or other pathway genes in zinc ions-treated cells. While zinc ions influx during platelet activation has been characterized[31], the direct action of physiological zinc ions concentrations on platelet aggregation and coagulation factor recruitment during thrombus formation has not been reported. Our *in vivo* experiments therefore address this gap by demonstrating that zinc ions directly increase bleeding volume, and we implicate migrasomes as a mediator of this effect.

In our cell-based assays, both $ZnSO_4$ and zinc gluconate inhibited migrasome formation at physiological concentrations (0-30 μmol/L). Notably, this suppression was evident even at 10 μmol/L and was sufficient to counteract the migrasome-promoting effect of TSPAN4 overexpression, indicating that zinc ions can effectively counteract migrasome biogenesis within their physiological range.

To verify that the inhibitory action requires intracellular zinc ions, we manipulated cellular zinc ions levels using disulfiram (which promotes zinc ions export via SLC30A transporters) and an anti-SLC39A6 antibody (which blocks zinc ions import)[20,21]. Reducing intracellular zinc ions in cells treated with either supplement restored migrasome numbers, confirming that the effect is mediated by internal zinc ions rather than extracellular interactions.

Zinc is required for platelet production, and both chronic and acute zinc deficiency impair platelet formation and coagulation[32,33]. Because migrasomes contribute to thrombus formation[15], the zinc ions-induced reduction in migrasomes might be expected to limit thrombosis. To test this *in vivo*, we administered a low dose of zinc ions intraperitoneally to mice. Within 24 h, circulating free migrasomes decreased markedly, and platelet counts and coagulation parameters were also altered, consistent with the idea that zinc ions-mediated suppression of migrasomes limits thrombus formation. However, translating this finding into an antithrombotic strategy faces several obstacles. Zinc ions have a narrow safety window. While adequate intake is essential, excess zinc ions can cause copper deficiency, gastrointestinal distress, and other adverse effects[34]. The antithrombotic efficacy of zinc has not been compared with that of established drugs such as aspirin, clopidogrel, or direct oral anticoagulants, and whether zinc supplementation offers any advantage in efficacy or safety is unknown. Further studies are needed to determine whether zinc can reach therapeutic concentrations at sites of thrombosis without systemic toxicity and to compare its effects directly with current clinical therapies.

Our study has several limitations. First, we did not validate the RNA-seq changes in autophagy, autophagosome, and mTOR signaling by Western blot for markers such as p-mTOR, p-p70S6K, microtubule-associated protein 1 light chain 3 (LC3)-I/II, and p62. These changes may be secondary to the zinc ions-induced reduction in ROS rather than direct drivers of migrasome inhibition. Second, zinc increased HMGCR activity, which is difficult to reconcile with the reduced cholesterol levels we observed, leaving the link between zinc ions and cholesterol suppression unresolved. Third, our cell-based assays relied on Huh7.5.1 cells, which are not endothelial in origin. Endothelial cells would provide a more physiologically relevant context for thrombosis. Fourth, only male mice were used, and sex differences in zinc metabolism and coagulation could affect the generalizability of our results. Fifth, we administered zinc intraperitoneally rather than orally, which does not fully mimic dietary intake. Finally, although we measured migrasome numbers, platelet counts, and bleeding volume, we did not use a direct thrombosis model. The conclusion that zinc suppresses thrombosis should therefore be considered preliminary and warrants further validation.

Conclusion

In summary, our data show that zinc ions regulate migrasome formation via cholesterol, sphingomyelin, and ROS, and that this regulation affects platelet function and thrombosis. These findings establish a connection between trace element homeostasis and migrasome-mediated hemostasis, and point to zinc ion modulation as a potential avenue for therapeutic intervention in thrombotic disorders. They also raise further questions about the interplay between zinc, cholesterol synthesis, and organelle biogenesis that merit additional study.

DECLARATIONS

Acknowledgments

The Graphical Abstract was created using Adobe Illustrator. We thank Yu L, Chisari FV, and Migrasome Therapeutics for providing the reagents.

Authors' contributions

Conceived and designed the study: Li A, Zhang L
Performed the investigation: Li A, Liu J, Zhu J
Developed the methodology and performed data analysis and interpretation: Li A
Prepared the visualizations: Li A, Zhang S
Wrote the original draft and reviewed and edited the manuscript: Li A, Zhang L
Obtained financial support: Zhang L
All authors read and approved the final manuscript.

Availability of data and materials

RNA-seq data were uploaded to GEO with the accession number GSE319187. The data underlying this article are available in the article and in its online Supplementary Materials.

AI and AI-assisted tools statement

During the preparation of this manuscript, the AI tool ChatGPT (version GPT-4o mini, released 2024-07-18) was used solely for language editing. The tool did not influence the study design, data collection, analysis, interpretation, or the scientific content of the work. All authors take full responsibility for the accuracy, integrity, and final content of the manuscript.

Financial support and sponsorship

This work was supported by the Taishan Scholars Program (No. tstp20221142) and the Joint Innovation Team for Clinical & Basic Research (No. 202409).

Conflicts of interest

All authors declared that there are no conflicts of interest.

Ethical approval and consent to participate

All animal experiments were conducted in accordance with the Regulations for the Administration of Affairs Concerning Experimental Animals of China. All animal experimental procedures were reviewed and approved by the Animal Ethics Committee of Shandong First Medical University (Approval No. W202504160624). All efforts were made to minimize animal suffering and reduce the number of animals used.

Consent for publication

Not applicable.

Copyright

© The Author(s) 2026.

Supplementary Materials

Supplementary Materials

REFERENCES

1. Chen B, Yu P, Chan WN, et al. Cellular zinc metabolism and zinc signaling: from biological functions to diseases and therapeutic targets. *Signal Transduct Target Ther.* 2024;9:6. DOI PubMed PMC
2. Camp OG, Bembenek JN, Goud PT, Awonuga AO, Abu-Soud HM. The implications of insufficient zinc on the generation of oxidative stress leading to decreased oocyte quality. *Reprod Sci.* 2023;30:2069-78. DOI PubMed PMC
3. Brito S, Heo H, Kim J, et al. Age-associated interplay between zinc deficiency and Golgi stress hinders microtubule-dependent cellular signaling and epigenetic control. *Dev Cell.* 2025;60:1304-20.e7. DOI PubMed
4. Vu TT, Fredenburgh JC, Weitz JI. Zinc: an important cofactor in haemostasis and thrombosis. *Thromb Haemost.* 2013;109:421-30. DOI PubMed
5. Mammadova-Bach E, Braun A. Zinc homeostasis in platelet-related diseases. *Int J Mol Sci.* 2019;20:5258. DOI PubMed PMC
6. Zhu T, Ubhayasekera W, Nickolaus N, et al. Zinc ions bind to and inhibit activated protein C. *Thromb Haemost.* 2010;104:544-53. DOI PubMed
7. Sen P, Sahoo S, Pendurthi UR, Rao LV. Zinc modulates the interaction of protein C and activated protein C with endothelial cell protein C receptor. *J Biol Chem.* 2010;285:20410-20. DOI PubMed PMC
8. Fatah K, Hessel B. Effect of zinc ions on fibrin network structure. *Blood Coagul Fibrinolysis.* 1998;9:629-35. DOI PubMed
9. Watson BR, White NA, Taylor KA, et al. Zinc is a transmembrane agonist that induces platelet activation in a tyrosine phosphorylation-dependent manner. *Metallomics.* 2016;8:91-100. DOI PubMed
10. Huo YN, Ekholm J, Hanahan DJ. A preferential inhibition by Zn2+ on platelet activating factor- and thrombin-induced serotonin secretion from washed rabbit platelets. *Arch Biochem Biophys.* 1988;260:841-6. DOI PubMed
11. Majidi RF, Mesgar AS, Milan PB. Surface-modified, zinc-incorporated mesoporous silica nanoparticles with improved antibacterial and rapid hemostatic properties. *Colloids Surf B Biointerfaces.* 2024;243:114132. DOI PubMed
12. Liao X, Ji P, Chi K, et al. Enhanced inhibition of protein disulfide isomerase and anti-thrombotic activity of a rutin derivative: rutin:Zn complex. *RSC Adv.* 2023;13:11464-71. DOI PubMed PMC
13. Ma L, Li Y, Peng J, et al. Discovery of the migrasome, an organelle mediating release of cytoplasmic contents during cell migration. *Cell Res.* 2015;25:24-38. DOI PubMed PMC
14. Huang Y, Zucker B, Zhang S, et al. Migrasome formation is mediated by assembly of micron-scale tetraspanin macrodomains. *Nat Cell Biol.* 2019;21:991-1002. DOI PubMed
15. Jiang D, Jiao L, Li Q, et al. Neutrophil-derived migrasomes are an essential part of the coagulation system. *Nat Cell Biol.* 2024;26:1110-23. DOI PubMed PMC
16. Li A, Yang C, Zhang L. Zinc oxide nanoparticles promote migrasomes formation. *J Hazard Mater.* 2025;490:137792. DOI PubMed
17. Andrew D, Gail R, Morag B, Kishor R. Recommended reference intervals for copper and zinc in serum using the US National Health and Nutrition Examination surveys (NHANES) data. *Clin Chim Acta.* 2023;546:117397. DOI PubMed
18. Devarshi PP, Mao Q, Grant RW, Hazels Mitmesser S. Comparative absorption and bioavailability of various chemical forms of zinc in humans: a narrative review. *Nutrients.* 2024;16:4269. DOI PubMed PMC
19. Chen L, Ma L, Yu L. WGA is a probe for migrasomes. *Cell Discov.* 2019;5:13. DOI PubMed PMC
20. Zhou Y, Feng M, Zhang L. Repurposing disulfiram: an innovative inhibitory approach against a broad spectrum of viruses. *Biochem Biophys Res Commun.* 2025;782:152596. DOI PubMed
21. Zhou Y, Huang G, Liu M, Zhang M, Wu B, Gu J. SLC30 (ZnT) and SLC39 (ZIP) zinc transporter families: from gatekeepers of zinc homeostasis to promoters of tumorigenesis and targets for clinical therapy. *Front Immunol.* 2025;16:1750534. DOI PubMed PMC
22. Hou Y, Li A, Zhang S, Zhao M, Zhang L. Dietary zinc ions inhibit virus-induced migrasome formation, potentially reducing viral transmission. *J Infect.* 2026;92:106685. DOI PubMed
23. Ding T, Ji J, Zhang W, et al. The phosphatidylinositol (4,5)-bisphosphate-Rab35 axis regulates migrasome formation. *Cell Res.* 2023;33:617-27. DOI PubMed PMC
24. Zhang N, Gao S, Zhang L. Chikungunya virus nsP1 induces migrasome formation. *J Infect.* 2022;85:e158-61. DOI PubMed
25. Lu P, Liu R, Lu D, et al. Chemical screening identifies ROCK1 as a regulator of migrasome formation. *Cell Discov.* 2020;6:51. DOI PubMed PMC
26. Wu Z, Gao D, Găman MA, Prabahar K, Kord-Varkaneh H, Yang Y. Association of dietary zinc intake with hs-CRP and the lipid profile: evidence from the 2017-2020 National Health and Nutrition Examination Survey (NHANES). *J Public Health Policy.* 2026;47:361-74. DOI PubMed
27. Loaiza-Giraldo JP, Amigo-Fierro F, Cancino-Castro CI, et al. Effects of zinc supplementation on glycemic control, insulin resistance, inflammation and oxidative stress in diabetes: a systematic review and meta-analysis of randomized controlled trials. *Endocrinol Diabetes Metab.* 2026;9:e70264. DOI PubMed PMC

28. Fowler DM, Cooper SJ, Stephany JJ, Hendon N, Nelson S, Fields S. Suppression of statin effectiveness by copper and zinc in yeast and human cells. *Mol Biosyst.* 2011;7:533-44. DOI PubMed PMC
29. Würtz P, Wang Q, Soininen P, et al. Metabolomic profiling of statin use and genetic inhibition of HMG-CoA reductase. *J Am Coll Cardiol.* 2016;67:1200-10. DOI PubMed PMC
30. Coupland CA, Naylor-Adamson L, Booth Z, et al. Platelet zinc status regulates prostaglandin-induced signaling, altering thrombus formation. *J Thromb Haemost.* 2023;21:2545-58. DOI PubMed
31. Kuravi SJ, Ahmed NS, Taylor KA, et al. Delineating zinc influx mechanisms during platelet activation. *Int J Mol Sci.* 2023;24:11689. DOI PubMed PMC
32. Prasad AS, Rabbani P, Abbasii A, Bowersox E, Fox MR. Experimental zinc deficiency in humans. *Ann Intern Med.* 1978;89:483-90. DOI PubMed
33. Gordon PR, Woodruff CW, Anderson HL, O'Dell BL. Effect of acute zinc deprivation on plasma zinc and platelet aggregation in adult males. *Am J Clin Nutr.* 1982;35:113-9. DOI PubMed
34. Dai X, Li J. Iron and other metal ions in human health and disease. *MedComm.* 2026;7:e71021. DOI PubMed PMC

Disclaimer/Publisher's Note: All statements, opinions, and data contained in this publication are solely those of the individual author(s) and contributor(s) and do not necessarily reflect those of OAE and/or the editor(s). OAE and/or the editor(s) disclaim any responsibility for harm to persons or property resulting from the use of any ideas, methods, instructions, or products mentioned in the content.


© The Author(s) 2026. Open Access This article is licensed under a Creative Commons Attribution 4.0 International License (https://creativecommons.org/licenses/by/4.0/), which permits unrestricted use, sharing, adaptation, distribution and reproduction in any medium or format, for any purpose, even commercially, as long as you give appropriate credit to the original author(s) and the source, provide a link to the Creative Commons license, and indicate if changes were made.